Emerging inverse energy transfer in finite-temperature superfluid vortex reconnections

P. Z. Stasiak, A. Baggaley, and C.F. Barenghi
School of Mathematics, Statistics and Physics, Newcastle University, Newcastle upon Tyne, NE1 7RU, United Kingdom

G. Krstulovic
Université Côte d'Azur, Observatoire de la Côte d'Azur, CNRS,Laboratoire Lagrangre, Boulevard de l'Observatoire CS 34229 - F 06304 NICE Cedex 4, France

L. Galantucci
Istituto per le Applicazioni del Calcolo "M. Picone" IAC CNR, Via dei Taurini 19, 00185 Roma, Italy
(Dated: November 5, 2024)

Lorem ipsum dolor sit amet, consectetuer adipiscing elit. Etiam lobortis facilisis sem. Nullam nec mi et neque pharetra sollicitudin. Praesent imperdiet mi nec ante. Donec ullamcorper, felis non sodales commodo, lectus velit ultrices augue, a dignissim nibh lectus placerat pede. Vivamus nunc nunc, molestie ut, ultricies vel, semper in, velit. Ut porttitor. Praesent in sapien. Lorem ipsum dolor sit amet, consectetuer adipiscing elit. Duis fringilla tristique neque. Sed interdum libero ut metus. Pellentesque placerat. Nam rutrum augue a leo. Morbi sed elit sit amet ante lobortis sollicitudin. Praesent blandit blandit mauris. Praesent lectus tellus, aliquet aliquam, luctus a, egestas a, turpis. Mauris lacinia lorem sit amet ipsum. Nunc quis urna dictum turpis accumsan semper.

Introduction.— Turbulence is a fundamental phenomenon that governs fluid motion across a vast range of scales, influencing everything from atmospheric dynamics to industrial processes. Understanding turbulence and the mechanisms of energy cascades is crucial for predicting flow behavior, optimizing performance, and advancing technologies in fields such as aerospace engineering, meteorology, and oceanography. In three-dimensional classical fluid dynamics, turbulence is often characterised by a forward cascade - a transfer of an inviscid, conserved quantity (typically energy) from large eddies to increasingly smaller eddies by nonlinear interactions of fluid elements, until dissipation occurs at the smallest length scales [1]. The distribution of energy across length scales in fluid dynamics is often referred to as the Kolmogorov spectrum, where the energy spectrum $E(k)$ scales according to $\sim k^{-5/3}$ at the intermediate length scales [2]. Confining turbulence to two-dimensions is fundamentally different: a dual cascade emerges of both energy and enstrophy. The interplay between the two quanties favours the generation and persistence of large scale coherent structures, resulting in energy transfer from small to large length scales - an inverse cascade.

Remarkably, fluids that have undergone Bose-Einstein condensation such as helium-4 and atomic condensates differ signifcantly from classical fluids, yet can still capture the same behaviour [3–5]. In such exotic fluids, quantum mechanics dominates the dynamics, leading to peculiar phenomena such as superfluidity (flow without viscosity) and quantisation of circulation in superfluid vortices [6]. Kolmogorov-like scaling laws in helium-4 have been observed experimentally both in mechanically generated turbulence [7] and thermally generated turbulence using counterflow channels [8]. Theoretical [9–11] and experimental [12, 13] work in quasi-two-dimensional atomic condensates also report the existence of an inverse energy cascade by small scale forcing.

In recent years the role of helicity has been highlighted in the generation of inverse energy transfers for three-dimensional turbulence, without the constraint of quasi-two-dimensionality [14, 15]. Statistically stationary inverse energy transfer has been sustained in a three-dimensional system by an imbalance of non-local homochiral modes through decimating certain triadic interactions [15], and more recently by a strong, external injection of positive helical modes at all length scales [16]. We will show that a chiral imbalance is a naturally occuring phenomenon in superfluids as a result of quantum vortex reconnection events. During such events, two superfluid vortices collide and exchange circulation, altering the overall topology [17, 18]. Punctuated energy injection resulting from the violent nature of vortex reconnections [19] pave the way for an imbalance of chirality by multi-scale energy injection.

In principle, to facilitate an inverse transfer of energy in a classical fluid requires a precise construction of conditions. In this Letter, we aim to show that an inverse energy transfer arises naturally in the normal fluid phase of superfluid helium-4 as a result of superfluid vortex reconnections, an intrinsic property of all superfluids. We will show that energy is injected at the small length scales immediately in the post reconnection regimes and moves towards larger length scales, increasing the integral length scale $\mathcal{L}_E$ of the normal fluid component. We provide an explanation of the inverse energy transfer by decomposing the velocity and mutual friction fields

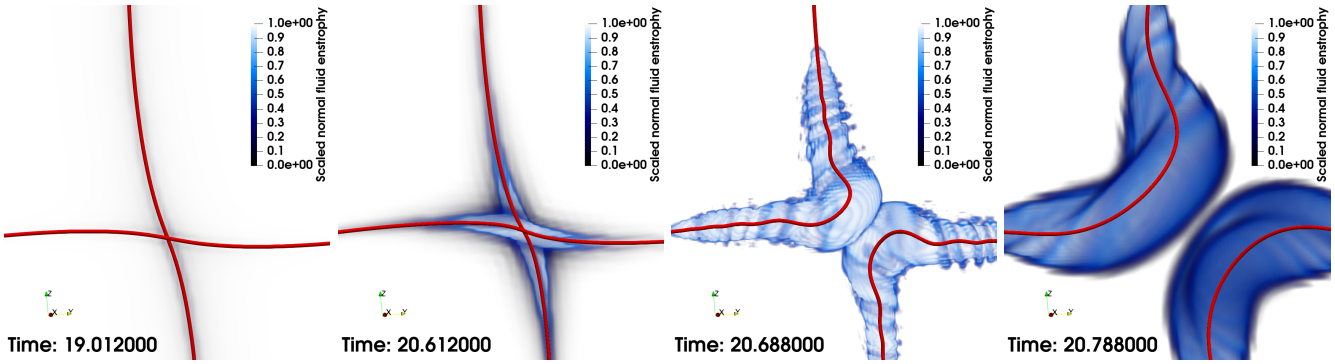

FIG. 1: 3D rendering of an orthogonal vortex configuration, undergoing a vortex reconnection. The red tube represents a superfluid vortex, where the radius has been greatly exaggerated for visual purposes, and the blue volume rendering represents the scaled normal fluid enstrophy $\boldsymbol{\omega}^2/\boldsymbol{\omega}^2_{max}$.

(the governing interaction force between the two-fluid components) into helical modes, showing that the imbalance of homochiral modes resulting from the punctuated energy and helicity injection during the reconnection process. Finally, we discuss the relevance of our findings to the broader field of transitions to superfluid turbulence.

Main results.— In this Letter, we use the Schwarz model [20] to parametrise superfluid vortex lines as space curves $\mathbf{s}(\xi, t)$, by assuming a large seperation of length scales between the vortex core $a_0 = 10^{-10}$m and the discretisation of vortex filaments $\Delta\xi$. Vortices are evolved according to

$$\dot{\mathbf{s}}(\xi,t) = \mathbf{v}_s + \frac{\beta}{1+\beta}\left[\mathbf{v}_{ns}\cdot\mathbf{s}'\right]\mathbf{s}' + \beta\mathbf{s}'\times\mathbf{v}_{ns} + \beta'\mathbf{s}'\times\left[\mathbf{s}'\times\mathbf{v}_{ns}\right], \tag{1}$$

where $\dot{\mathbf{s}} = \partial\mathbf{s}/\partial t$, $\mathbf{s}' = \partial\mathbf{s}/\partial\xi$ is the unit tangent vector, $\mathbf{v}_n$ and $\mathbf{v}_s$ are the normal fluid and superfluid velocities at $\mathbf{s}$, $\mathbf{v}_{ns} = \mathbf{v}_n - \mathbf{v}_s$, and β, β' are temperature and Reynolds number dependent mutual friction coefficients [21].The calculation of the superfluid velocity $\mathbf{v}_s$ is standard (see SM [22]) The normal fluid is described classically using the incompressible ($\nabla\cdot\mathbf{v}_n = 0$) Navier-Stokes equation:

$$\frac{\partial\mathbf{v}_n}{\partial t} + (\mathbf{v}_n\cdot\nabla)\mathbf{v}_n = -\frac{1}{\rho}\nabla p + \nu_n\nabla^2\mathbf{v}_n + \frac{\mathbf{F}_{ns}}{\rho_n} \tag{2}$$

where $\mathbf{F}_{ns}$ is the coupling mutual friction force, $\rho = \rho_n + \rho_s$, where ρ_n and ρ_s are the normal fluid and superfluid densities, p is the pressure and ν_n is the kinematic viscosity of the normal fluid. We define the mutual friction force $\mathbf{F}_{ns}$ as the line integral of the mutual friction per unit length $\mathbf{f}_{ns}$ (see SM [22]),

$$\mathbf{F}_{ns}(\mathbf{x}) = \oint_{\mathcal{L}} \delta(\mathbf{x}-\mathbf{s})\mathbf{f}_{ns}(\mathbf{s})d\xi \tag{3}$$

where $\mathcal{L}$ represents the entire vortex geometry. The regularisation of mutual friction is performed using a physically self-consistent scheme [21, 23, 24].

We set two pairs of orthogonal vortices, where corresponding vortices in each pair have oppposite circulation in order to preserve superfluid periodicity along the boundaries, and we consider two distinct temperatures, $T = 1.9K$ and $T = 2.1K$. Vortex pairs are seperated by distance D_ℓ, and each vortex within each pair is seperated by distance d_ℓ, such that $d_\ell \ll D_\ell$. The seperation of scales ensures that the dynamics in the vicinity of the reconnection are dominated by local interactions, and that far-reaching contributions from the

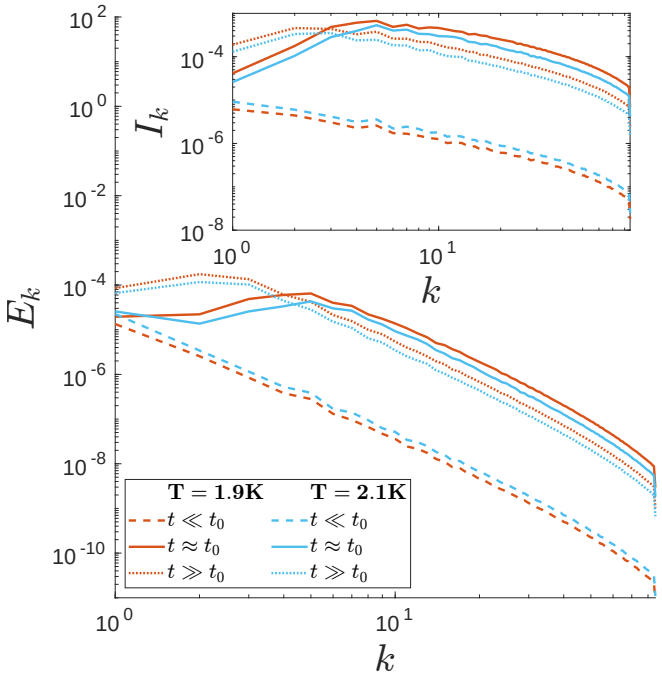

FIG. 2: Normal fluid kinetic energy spectrum E_k before reconnection (dashed lines), at reconnection (solid lines) and after reconnection (dotted lines) for $T = 1.9K$ and $T = 2.1K$. *Inset:* Mutual friction injection spectrum I_k at the same snapshots in time.

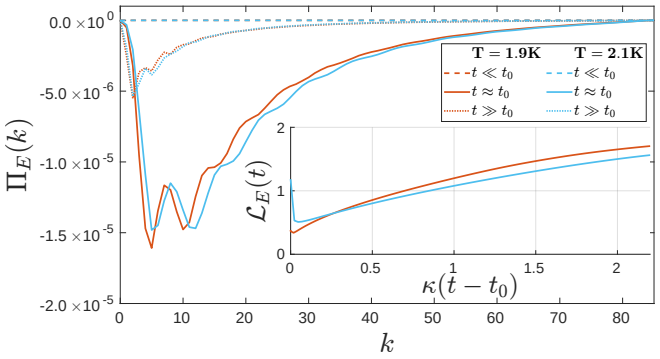

FIG. 3: *Top:* Mutual friction injection spectrum I_k. *Bottom:* Spectral normal fluid kinetic energy flux Π_E. *Inset:* Post reconnection evolution of the integral length scale $\mathcal{L}_E$.

other vortex pair are neglible. The evolution of the vortex reconnection of a single pair is reported in Fig. 1.

During vortex reconnections, energy is injected into the normal fluid at the small length scales in a natural way in the absence of external property, an intrinsic and unique feature of quantum fluids. The injection of energy is clear in the kinetic energy spectrum E_k which is shown in in Fig. 2, at wavenumbers $k > 10$ a vast increase can be observed $E_k(t \approx t_0)/E_k(t \ll t_0) \sim 10^2$, evidence of very strong energy injection. Remarkably, in the post reconnection regime E_k appears to increase when k is small, and decay at large values of k, suggesting a possible mechanism by which energy generated at small length scales is transferred to larger scales. The energy spectrum E_k evolves according to the balance sources/sinks and internal transfers,

$$\frac{\partial E_k}{\partial t} = T_k - D_k + I_k \tag{4}$$

where T_k is the spectral kinetic energy transfer function, $D_k = 2\nu_n k^2 E_k$ is the dissipation spectrum and $I_k = \mathrm{Re}(\hat{\mathbf{F}}_{ns}(\mathbf{k}) \cdot \hat{\mathbf{v}}^*(\mathbf{k}))$ is the injection spectrum due to the mutual friction $\mathbf{F}_{ns}$. Abrupt changes in the topology of vortex lines, such as during vortex reconnections, form highly curved cusps, which then relaxes in structures with small radii of curvature. As $F_{ns} \propto |\mathbf{v}_l - \mathbf{v}| \approx |\mathbf{v}_l| \propto 1/R_c$, the scale of energy injection is small as R_c is also small during injection. This can be seen in Fig. 2. As time evolves, the smallest perturbations are damped by friction the fastest, resulting in the peak of the injectrum spectrum I_k to shift towards the larger length scales. The injection spectrum I_k as shown in the inset of Fig. 3 again shows that the injection of energy covers primarily the high k range, but is not limited to a thin band of injection. In fact, the energy flux $\Pi_E(k) = \int_k^\infty T_k dk$ as shown in Fig. 3 asserts a hallmark feature of inverse energy cascades, typical in 2D isotropic turbulence. A flux of $\Pi_E(k) < 0$ implies a negative flux of energy from small to large k, i.e. an inverse transfer of energy. The effect of kinetic energy transferral to large length scales results in the creation of large scale structures, evident in the evolution of the integral length scale $\mathcal{L}_E$, where

$$\mathcal{L}_E = \frac{\pi}{2\langle \mathbf{v}'^2 \rangle} \int_0^\infty \frac{E_k}{k} dk \tag{5}$$

and $\langle \mathbf{v}'^2 \rangle$ represents the turbulent kinetic energy. In the inset of Fig. 3, $\mathcal{L}_E$ steadily increases in the post-reconnection region, implying a generation of large scale structure.

In order to explain the inverse energy transfer mechanism, we look for a chirality unbalance as a result of the reconnection process. we follow recent work in classical fluids outlined in Refs. [15, 16], where it is even possible to sustain an inverse energy cascade under a helical forcing applied at all length scales. Typically, velocity coefficients $\hat{\mathbf{v}}(\mathbf{k})$ can be decomposed into their helical modes, where $\hat{\mathbf{v}}(\mathbf{k}) = v^+(\mathbf{k})\mathbf{h}^+(\mathbf{k}) + v^-(\mathbf{k})\mathbf{h}^-(\mathbf{k})$ and satisfies $\mathbf{k} \cdot \hat{\mathbf{v}}(\mathbf{k}) = 0$, where $\mathbf{v}^\pm$ are complex scalars and $\mathbf{h}^\pm(\mathbf{k})$ are the two eigenvectors of the curl operator, such that $i\mathbf{k} \times \mathbf{h}^\pm(\mathbf{k}) = \pm k\mathbf{h}^\pm(\mathbf{k})$. To explain the inverse energy transfer in terms of helical modes, we show that in fact the driving force, which in our case is a punctuated burst due to superfluid vortex reconnections, is of a helical nature. The mutual friction modes $\hat{\mathbf{F}}_{ns}(\mathbf{k})$ are not incompressible, and so we take the projection of the modes orthogonal to the wavenumber $\mathbf{k}$. The projected modes $\hat{\mathbf{f}}(\mathbf{k})$ are then decomposed into helical modes $\hat{\mathbf{f}}(\mathbf{k}) = f^+\mathbf{h}^+(\mathbf{k}) + f^-\mathbf{h}^-(\mathbf{k})$. The ratio of the two helical modes $|f^+|^2/|f^-|^2$ are shown in Fig. 4. At reconnection time t_0, the ratio is much larger, indicating that indeed this force is chiral and that a clear inbalance that favours the injection of positive helical modes, changing the chirality of the flow (as seen in Fig. 4). In the same way, helicity modes $\hat{\mathcal{H}}(\mathbf{k})$ can be decomposed,

$$\hat{\mathcal{H}}(\mathbf{k}) = k(E^+(\mathbf{k}) - E^-(\mathbf{k})) = \mathcal{H}^+ + \mathcal{H}^- \tag{6}$$

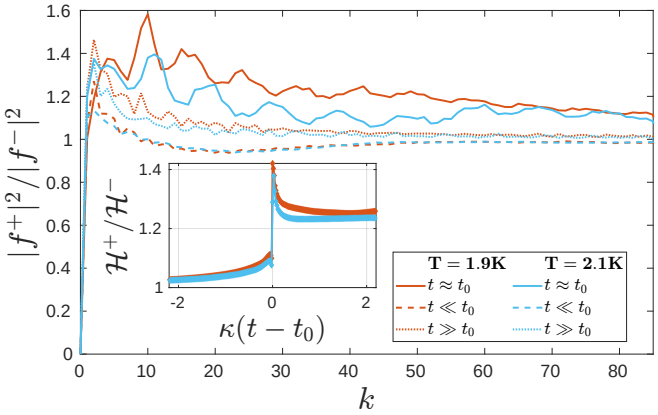

FIG. 4: The ratio of the projected helical mutual friction modes $f^+(k)$ and $f^-(k)$

where $E^{\pm} = \frac{1}{2}|\mathbf{v}^{\pm}(\mathbf{k})|^2$ are the helical energy modes. The evolution of the ratio $\mathcal{H}^+/\mathcal{H}^-$ is shown in the inset of Fig. 4. The sharp increase at reconnection time t_0 is evidence of a large influx of positive helical modes as a result of the vortex reconnection, which is in agreement with the conditions to facilitate an inverse energy transfer by a helical injection. Finally, as observed in Ref. [16], it is necessary for the forcing to cover the entire spectrum of k, which from the inset of Fig. 2, it is evident that this indeed the case.

Closing remarks.— ...

[1] L. F. Richardson, *Weather prediction by numerical process* (University Press, 1922).

[2] U. Frisch, Turbulence: The Legacy of A. N. Kolmogorov (1995).

[3] J. Maurer and P. Tabeling, Local investigation of superfluid turbulence, EPL **43**, 29 (1998).

[4] A. W. Baggaley, L. K. Sherwin, C. F. Barenghi, and Y. A. Sergeev, Thermally and mechanically driven quantum turbulence in helium II, Phys Rev B **86**, 104501 (2012).

[5] L. K. Sherwin-Robson, C. F. Barenghi, and A. W. Baggaley, Local and nonlocal dynamics in superfluid turbulence, Phys. Rev. B **91**, 104517 (2015).

[6] C. Barenghi and Y. Sergeev, *Vortices and turbulence at very low temperatures*, Vol. 501 (Springer Science & Business Media, 2009).

[7] J. Salort, C. Baudet, B. Castaing, B. Chabaud, F. Daviaud, T. Didelot, P. Diribarne, B. Dubrulle, Y. Gagne, F. Gauthier, *et al.*, Turbulent velocity spectra in superfluid flows, Physics of Fluids **22** (2010).

[8] J. Gao, E. Varga, W. Guo, and W. Vinen, Energy spectrum of thermal counterflow turbulence in superfluid helium-4, Physical Review B **96**, 094511 (2017).

[9] A. S. Bradley and B. P. Anderson, Energy spectra of vortex distributions in two-dimensional quantum turbulence, Physical Review X **2**, 041001 (2012).

[10] M. T. Reeves, T. P. Billam, B. P. Anderson, and A. S. Bradley, Inverse Energy Cascade in Forced Two-Dimensional Quantum Turbulence, Phys. Rev. Lett. **110**, 104501 (2013).

[11] T. Simula, M. J. Davis, and K. Helmerson, Emergence of order from turbulence in an isolated planar superfluid, Phys. Rev. Lett. **113**, 165302 (2014).

[12] S. P. Johnstone, A. J. Groszek, P. T. Starkey, C. J. Billington, T. P. Simula, and K. Helmerson, Evolution of large-scale flow from turbulence in a two-dimensional superfluid, Science **364**, 1267 (2019).

[13] G. Gauthier, M. T. Reeves, X. Yu, A. S. Bradley, M. A. Baker, T. A. Bell, H. Rubinsztein-Dunlop, M. J. Davis, and T. W. Neely, Giant vortex clusters in a two-dimensional quantum fluid, Science **364**, 1264 (2019).

[14] Q. Chen, S. Chen, and G. L. Eyink, The joint cascade of energy and helicity in three-dimensional turbulence, Physics of Fluids **15**, 361 (2003).

[15] L. Biferale, S. Musacchio, and F. Toschi, Inverse Energy Cascade in Three-Dimensional Isotropic Turbulence, Phys. Rev. Lett. **108**, 164501 (2012).

[16] F. Plunian, A. Teimurazov, R. Stepanov, and M. K. Verma, Inverse cascade of energy in helical turbulence, Journal of Fluid Mechanics **895**, A13 (2020).

[17] A. Villois, D. Proment, and G. Krstulovic, Irreversible dynamics of vortex reconnections in quantum fluids, Physical Review Letters **125**, 164501 (2020).

[18] S. Zuccher, M. Caliari, A. W. Baggaley, and C. F. Barenghi, Quantum vortex reconnections, Physics of fluids **24** (2012).

[19] Ref to first reconnection paper on arxiv.

[20] KW. Schwarz, Three-dimensional vortex dynamics in superfluid ^{4}He, Phys. Rev. B **38**, 2398 (1988).

[21] L. Galantucci, A. W. Baggaley, C. F. Barenghi, and G. Krstulovic, A new self-consistent approach of quantum turbulence in superfluid helium, Eur. Phys. J. Plus **135**, 547 (2020).

[22] See supplementary materials.

[23] P. Gualtieri, F. Picano, G. Sardina, and C. M. Casciola, Exact regularized point particle method for multiphase flows in the two-way coupling regime, Journal of Fluid Mechanics **773**, 520 (2015).

[24] P. Gualtieri, F. Battista, and C. M. Casciola, Turbulence modulation in heavy-loaded suspensions of tiny particles, Physical Review Fluids **2**, 034304 (2017).